







## Research Article

## Bio-Convective Thermally Radiated Casson Fluid Model PDEs Past over a Darcy-Forchheimer Porous Stretched Sheet via OHAM Strategy

Syed Tehseen Abbas <sup>1</sup>, , Shah Jahan <sup>1</sup>, , Arsalan Afzal <sup>1</sup>, , Muhammad Sohail <sup>1,\*</sup>, <sup>1</sup> Institute of Mathematics, Khwaja Fareed University of Engineering & Information Technology, Rahim Yar Khan 64200, Pakistan.

## ARTICLE INFO

## Article History

Received 28 Feb 2024

Revised: 29 Apr 2024

Accepted 28 May 2024

Published 20 Jun 2024

## Keywords

Casson Nanofluid

Darcy-Forchheimer

Thermal Radiation

Brownian motion

Thermophoresis



## ABSTRACT

The current study examines the topic of continuous flow of nanofluids over two-directional boundary level employing Casson heat transmission across a linearly stretched sheet. Firstly, the partial differential equations are transformed into non-linear ordinary differential equations with the help of similarity parameters. These non-linear ordinary differential equations are solved with the given boundary conditions by applying the BVPh2.0 method on Mathematica software. The effects of magnetic impact, radiation parameter, porosity number, Brownian motion parameter, thermophoresis parameter, Casson fluid parameter, Schmidt number, Prandtl number, pecelet number, bioconvection on Velocity, temperature and concentration profiles is observed. It is noted that the concentration and temperature profiles increase by expanding values of thermophoresis parameter also the temperature increase by increment in Brownian motion while a reverse result obtained on concentration profile. Also, the influence of Casson fluid, thermophoresis and Brownian motion on skin friction, Sherwood number and Nusselt number is noted and check the behavior of these numbers by increasing or decreasing values of thermophoresis parameter, Casson fluid parameter and Brownian motion. And, calculated that by increment in thermophoresis and Brownian motion, the Nusselt number decreases. The graphs of temperature profile, velocity profile and concentration profile are drawn and also other results are tabulated.

## 1. INTRODUCTION

Nanofluids are frequently used as heat transmission fluids in heat transfer tools due to their enlarged thermal properties, such as temperature exchangers, industrialized cooling systems (similar to plane panel), and radiators. Casson liquefied notion for the movement of deformable liquors was prepared by Casson [1]. Casson fluid is strain liquefied that have immeasurable viscous at zero shear rates and zero viscidness at infinite shear rates, constructing stress through which no flow happens. Soups, jelly, sauce, and honey are a limited sample of Casson fluid. The Casson nanofluid terminated as non-linear disposed elastic sheet through Soret also Dufour belongings and the growing demands on behalf of non-Newtonian nanofluid streams in industrial and manufacturing pitches. Buongiorno [2] idea of heat effectiveness of liquid runs in the existence of Brownian research and thermal features served as foundation aimed at the model engaged in this analysis. By taking into account vital flow characteristics of the exaggerated boundary sheet, the Casson fluid movement matter lengthways an inclined channel is displayed for pick up more about the heat and mass conversation phenomena.

Numerous efforts have been made in recent years to study the nanofluid due to its exceptional thermodynamic characteristics. The industrial and nanotechnology industries have greatly benefited from recent advances in nanofluids and related mathematical modelling. Nanofluids can used to cool vehicle motors, biomedical applications, laundry washers, diode arrays of different welding frameworks, etc. Haddad et al. [3] elaborated on free convection in nanoliquids by taking into explanation the Rayleigh-Bernard issue as well as the effects of thermophoresis and Brownian motion. By employing the DTM Sheikholeslami and Ganji [4] quantitatively evaluated nanofluid heat exchange and flow between parallel plates while taking into account Brownian motion. Hayat et al. [5] have presented the magnetohydrodynamic (MHD) flow towards a penetrable stretching geometry in the presence of nanoparticles under the effect of Brownian motion. Effects of Brownian motion and Thermophoresis were used by Babu and Sandeep [6] to describe 3D MHD slip flow over a narrow stretched sheet. Malvandi et al. [7] observed the migration of nanoparticles increase in heat transmission nearby the film layer of nanofluids via a vertical tube while taking the thermophoresis effect into consideration. The conclusion of thermal

\*Corresponding author. Email: [it@gmail.com](mailto:it@gmail.com)

radiation and heat transmission effects of nanoparticle movement over a sheet under consideration of Brownian motion, was developed by Dogonchi and Ganji [8]. Ullah et al. [9] also took into account other fascinating studies on nanofluid flow together with the Reiner-Philippoff fluid model. The earliest dynamic hypothesis of Brownian motion was put out by Nelson [10].

Casson fluid is a plastic fluid with constitutive equations that generate shear stress. It is specific kind of non-Newtonian fluid that shows elastic solid-like behavior. To examine the Casson boundary layer approaching the stagnation point on a stretched surface, Mustafa et al. [11] employed the homotopy analysis technique. While, to identify various characteristics transfer of heat in Casson nanofluid, many authors [12-15] have employed both viscous dissipation conditions and Joule heating. According to Ojjela et al. [16] Casson fluid investigations amid parallel disc renewals showed the irreversibility distribution was diminished by the dissipation effect. An experiment of Casson nanofluid past the landing surface was conducted by Rafique et al. [17]. They observed the Soret and Dufour effects on an inclined extending surface, along with the impacts of a Casson nanofluid boundary layer flow. Rafique et al. [18] used the Keller box solving approach in another study to evaluate how chemical reactions and magnetic forces affect Casson nanofluid modelling. Analytical methods were employed by Abolbashari et al. [19] to investigate generational entropy of Casson nanofluid along an extrusion surface. Sreenivasulu et al. [20] investigated the Casson nanofluid characteristics by taking into account magnetic field and a stretched porous sheet. It shown that increasing the magnetic force improves mass transferal while decreasing heat transport. Non-linear radiation in bio-convective Casson nanofluid explored by Oyelakin et al. [21]. The idea of Pulsatile Casson fluid flow across a stenosis bifurcation route was offered by Shaw et al. [22]. Shahzad et al. [23] have discovered the swirling Darcy-Forchheimer of Casson hybrid nanofluid flow. They applied parallel plates to the channel flow and the degree to which porosity, the nature of viscous fluids, rotational coordinates, and magnetic interactions affected thermal properties was recorded. Mehmood et al. [24] explained the joint effects of mixed convection on oblique Casson fluid across a stretched sheet. The Casson fluid due to magnetic field and stretchable cylinder was presented by Taimoor et al. [25]. A study of Micropolar Casson with internal heating over a stretched sheet done by Mehmood et al. [26]. Their theoretical investigation looks at the impact of micro-rotation on mixed convective flow.

In machining tasks including grinding, spinning, and crushing, nanofluids are used. Investigators have sustained their efforts to make important influences to nanofluid with the interruption of varied nanoparticles, mainly in this period. The nanofluid flow over the turning cone was explored by Hussain et al. [27]. Prasannakumara [28] using the Cattaneo-Cristov thermal incline thought, the clarifications for ferromagnetic fluid movement on an elastic surface were evaluated. Shukla and Rana [29] analyzed the movement of nanoparticles on the sheet. Amjad et al. [30] calculated the Micropolar Casson movement of fluid at curved surface. They spoke about connections of Brownian and thermophoretic gesture with induced magnetic hydrodynamics. Lanjwani et al. [31] examined Casson nanofluid triple keys at the perpendicular nonlinear stretching sheet. Mahanthesh and Joseph [32] examined the characteristics of non-Newtonian fluids of 3rd grade using thermophoresis and Brownian motion influences. Mabood and Shateyi [33] have studied how time-dependent MHD flow impacted a permeable overextended sheet.

MHD (magneto-hydrodynamics) Casson nanofluid is a kind of fluid that combines the properties of Casson fluid, a magnetic field, and the attendance of nanoparticles. MHD Casson nanofluid is a complex fluid system that has potential applications in several fields, counting energy transport, cooling, and biomedical manufacturing. Haq et al. [34] examined the effects of heat and MHD transmission on Casson nanofluid flow across a contracting sheet. Shah et al. [35] presented the generation of entropy across nonlinearly expanding surface. MHD Casson fluid along with production of entropy and hall influences over stretching sheet, studied by Abd El-Aziz and Afify [36]. Ali et al. [37] explored the generation of entropy in MHD mixed-convective Casson nanofluid across nonlinear stretchable sheet. Metri et al. [38] investigated the MHD Casson with convective boundary conditions along a velocity slip over nonlinear stretching sheet. Souayah et al. [39] observed the MHD Casson and radiative heat transmission. The idea of MHD 3D Casson fluids across a permeable linearly stretched sheet was suggested by Nadeem et al. [40]. By using stretching sheet Wang et al. [41] discussed the activation energy on 3D Casson nanofluid motion. By applying a convective boundary condition Nadeem et al. [42] were able to better understand mass and heat transmission of a 3D MHD Casson nanofluid and structured the warm fluid along the bottom surface of wall. The 3D Casson fluid was examined by Mahanta et al. [43]. The similarity solution of a three-dimensional Casson nanofluid across stretched surface was detected by Sulochana et al. [44]. The influence of slip and convective limit conditions on MHD stagnation point and thermal exchange caused by Casson nanofluid across a stretched sheet is examined by g. Ibrahim and Makinde, [45]. 3D presenting of MHD bio-convective Casson nanofluid with heat source and gyrotactic micro-organisms over exponential stretching sheet, described by Makkar et al. [46].

## 2. PROBLEM FORMULATION

Considered a viscid nanofluid passes over a flat stretching surface as shown in Fig. 1 and flow is incompressible, laminar, steady, two-dimensional boundary layer that corresponds to  $y = 0$  plane. The flow is limited by  $y$  greater than 0. Expanding the sheet while applying two same opposite pressures along the  $x$ -direction concurrently produces flow. If origin is fixed, the sheet will expand at rate of  $u_w(x) = \alpha x$ , wherever  $x$  is the coordinate acquired by crossing linear extending plate and denotes a "constant."

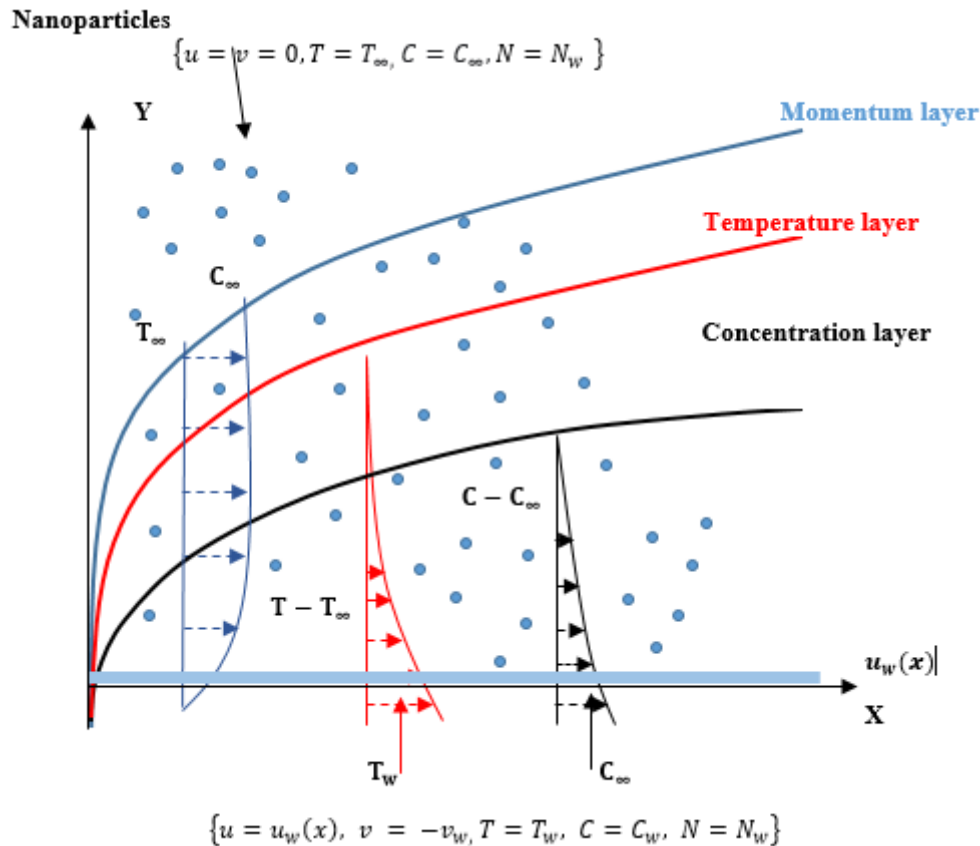


Fig. 1. Flow Diagram.

At stretching surface, temperature  $T$  and nanoparticles concentration  $C$  are thought to be constants,  $T_w$  and  $C_w$ . The ambient temperature  $T$  and nanoparticles concentration  $C$  represented by  $T_\infty$  and  $C_\infty$  if  $y$  tends to be infinite. The following formulas, which operate on the linear stretching sheet's flow and heat transmission appearances approximately inside boundary layer, are used in both cases.

$$\frac{\partial u}{\partial x} + \frac{\partial v}{\partial y} = 0, \tag{1}$$

$$u \frac{\partial u}{\partial x} + v \frac{\partial u}{\partial y} = \nu \left( 1 + \frac{1}{\beta} \right) \frac{\partial^2 u}{\partial y^2} - \left( \frac{\nu}{K_1} + \frac{C_b}{x\sqrt{K_1}} u \right) u - \frac{\sigma B_0^2}{\rho} u, \tag{2}$$

$$u \frac{\partial T}{\partial x} + v \frac{\partial T}{\partial y} = \alpha \frac{\partial^2 T}{\partial y^2} + \tau \left\{ D_B \left( \frac{\partial C}{\partial y} \cdot \frac{\partial T}{\partial y} \right) + \frac{D_T}{T_\infty} \left( \frac{\partial T}{\partial y} \right)^2 \right\} - \frac{1}{\rho c} \frac{\partial q_r}{\partial y} + \frac{Q(x)}{\rho c_p} (T - T_\infty), \tag{3}$$

$$u \frac{\partial C}{\partial x} + v \frac{\partial C}{\partial y} = D_B \frac{\partial^2 C}{\partial y^2} + \frac{D_T}{T_\infty} \frac{\partial^2 T}{\partial y^2}, \tag{4}$$

$$v \frac{\partial N}{\partial y} + u \frac{\partial N}{\partial x} = D_m \frac{\partial^2 N}{\partial y^2} + \frac{bW_c}{C_w - C_\infty} \frac{\partial}{\partial y} \left( N \frac{\partial C}{\partial y} \right), \tag{5}$$

For boundary conditions:

$$u = u_w(x), \quad v = -v_w, \quad T = T_w, \quad C = C_w, \quad N = N_w, \quad \text{at } y = 0, \tag{6}$$

$$u = v = 0, \quad T = T_\infty, \quad C = C_\infty, \quad N = N_\infty, \quad \text{as } y \rightarrow \infty. \tag{7}$$

And the stream function is  $\Psi = (av)^{1/2}xf(\eta)$  and for values of u and v we have:

$$u = \frac{\partial\Psi}{\partial y}, \quad v = -\frac{\partial\Psi}{\partial x}, \tag{8}$$

$$u = axf'(\eta), \quad v = -\left(\frac{a\mu}{\rho}\right)^{\frac{1}{2}}f(\eta). \tag{9}$$

And, here are some similarity transformations given below:

$$\eta = \left(\frac{a}{v}\right)^{1/2}y, \tag{10}$$

$$\theta(\eta) = \frac{T - T_\infty}{T_w - T_\infty}, \quad \Phi(\eta) = \frac{C - C_\infty}{C_w - C_\infty}, \quad \chi(\eta) = \frac{(N - N_\infty)}{(N_w - N_\infty)}. \tag{11}$$

After solving the above equations by the help of similarity conversions, the equations takes the form:

$$\left(1 + \frac{1}{\beta}\right)f'''(\eta) - f'^2(\eta)(F_r + 1) + f(\eta)f''(\eta) - F'(M^2 + \lambda) = 0, \tag{12}$$

$$\left(1 + \frac{4}{3}Rd\right)\theta''(\eta) + PrNb\phi'(\eta)\theta'(\eta) + PrNt\theta'^2(\eta) + PrQ_0\theta(\eta) = 0, \tag{13}$$

$$\Phi''(\eta) + S_c f(\eta)\Phi'(\eta) + \frac{Nt}{Nb}\theta''(\eta) = 0, \tag{14}$$

$$\chi''(\eta) + LbF(\eta)\chi'(\eta) + Pe[\{\chi(\eta) + \omega\}\phi''(\eta) + \chi'(\eta)\phi'(\eta)] = 0. \tag{15}$$

Also, the boundary conditions becomes:

$$f'(0) = 1, f(0) = f_w, \theta(0) = 1, \Phi(\infty) = 0, \chi(0) = 1, \quad \text{at } \eta \rightarrow 0, \tag{16}$$

$$f'(\infty) = 0, f(\infty) = 0, \theta(\infty) = 0, \Phi(\infty) = 0, \chi(\infty) = 0, \quad \text{at } \eta \rightarrow \infty. \tag{17}$$

Here,  $\theta(\eta)$  denotes the temperature,  $f$  denotes velocity,  $\Phi(\eta)$  denotes nanoparticle’s concentration and  $\chi(\eta)$  gyrotactic microorganisms.

Where,

$$Pr = \frac{v}{\alpha}, \quad S_c = \frac{v}{D_B}, \quad Nb = \frac{(\rho c)_p D_B}{(\rho c)_f v} (C_w - C_\infty), \quad Nt = \frac{(\rho c)_p D_T (T_w - T_\infty)}{(\rho c)_f T_\infty v},$$

$$\omega = \frac{N_\infty}{(N_w - N_\infty)}, \quad Rd = \frac{4\sigma_{sb}T_\infty^3}{k_f k_{ABS}}, \quad \lambda = \frac{v}{aK_1}, \quad M = \sqrt{\frac{\sigma}{\rho a}} B_o,$$

$$F_r = \frac{C_b}{\sqrt{K_1}}, \quad P_r = \frac{v}{\alpha}, \quad Lb = \frac{v}{D_m}, \quad Pe = \frac{bW_c}{D_m}.$$

Skin Friction ( $C_f$ ), Nusselt number ( $Nu_x$ ) and Sherwood number ( $Sh_x$ ) are given as:

$$C_f = -\frac{\tau_w}{\rho u_w^2}, \quad Nu_x = \frac{xq_w}{K(T_w - T_\infty)}, \quad Sh_x = \frac{xq_m}{D_B(-C_\infty)}. \tag{18}$$

Where,  $\tau_w$  is stress of wall,  $q_w$  is heat flux at wall,  $q_m$  is flux of mass are set by:

$$\tau_w = \rho\nu \left(\frac{\partial u}{\partial y}\right)_{y=0}, \quad q_w = -k \left(\frac{\partial T}{\partial y}\right)_{y=0}, \quad q_m = -D_B \left(\frac{\partial \phi}{\partial y}\right)_{y=0}. \tag{19}$$

$$C_f Re_x^{1/2} = f''(0), \tag{20}$$

$$Re_x^{-1/2} . Nu_x = -\theta'(0), \tag{21}$$

$$Re_x^{-1/2} . Sh_x = -\varphi'(0). \tag{22}$$

Where  $Re_x$  is known as Reynolds number. It tells the kind of flow laminar or turbulent when the fluid flowing through the surface.

### 3. METHODOLOGY

There are many methods to deal non-linear ordinary differential equations but, in this paper, the adopted method is BVP4c on Mathematica software [47-50] to solve non-linear ODE's (12-15) with boundary conditions (16 & 17).

$$f_0 = 1 - e^{-\eta}, \theta_0 = e^{-\eta}, \varphi_0 = e^{-\eta}, \chi_0 = e^{-\eta} \tag{23}$$

$$\widehat{\zeta}_f = f''' - f', \widehat{\zeta}_\theta = \theta'' - \theta, \widehat{\zeta}_\varphi = \varphi'' - \varphi, \widehat{\zeta}_\chi = \chi'' - \chi. \tag{24}$$

And subsequent hypothesis,

$$\begin{aligned} \widehat{\zeta}_f &= [L_1 e^{-\eta} + L_2 e^{\eta} + L_3] = 0, \widehat{\zeta}_\theta = [L_4 e^{-\eta} + L_5 e^{\eta}] = 0, \widehat{\zeta}_\varphi = [L_6 e^{-\eta} + L_7 e^{\eta}] = 0, \widehat{\zeta}_\chi \\ &= [L_8 e^{-\eta} + L_9 e^{\eta}] = 0 \end{aligned} \tag{25}$$

### 4. RESULTS AND DISCUSSION

The influences of different parameters on variant profiles are debated here. The result of Casson parameter on velocity profiles is noted that results reduction in velocity profile in fig (1). It is observed by growing the Casson fluid factor ( $\beta$ ) the fluid viscosity increase results decrease in velocity. Fluid acts like shear-thickening in response to an incremental change in, which reduces fluidity and thickness of the momentum layer. In figs. (2-4), the velocity decrease as increase in values of local inertia, magnetic and porosity parameter

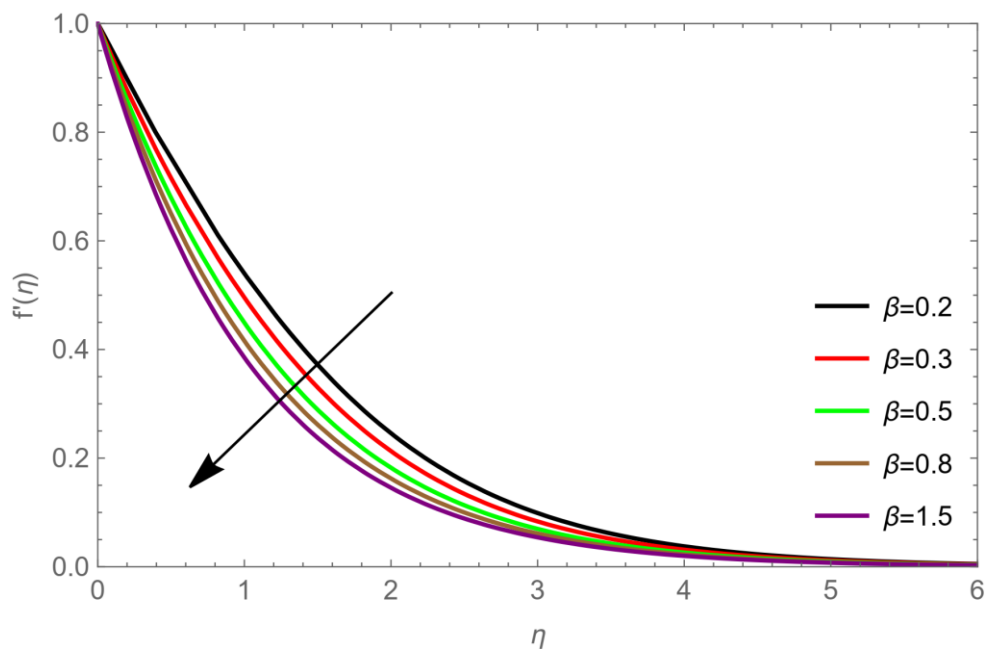


Fig. 1. Casson fluid parameter ( $\beta$ ) impact on velocity profiles for values  $Pr = 1.0, S_c = 0.2, Nb = 0.1, Nt = 0.2, M = 0.2, \omega = 0.2, \lambda = 0.1, Pe = 0.3, Rd = 0.2, F_r = 0.5, L_b = 0.2, Q_0 = 0.2$ .

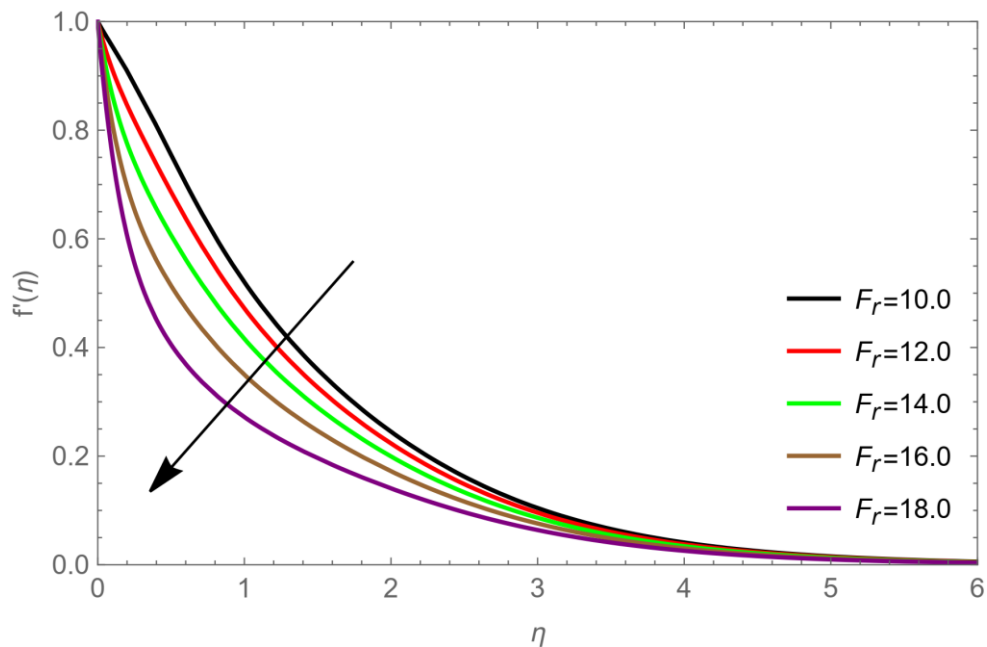


Fig. 2. Local inertia ( $F_r$ ) effects on velocity profiles for values  $Pr = 1.0, S_c = 0.2, Nb = 0.1, Nt = 0.2, M = 0.2, \omega = 0.2, \lambda = 0.1, Pe = 0.3, Rd = 0.2, \beta = 0.5, L_b = 0.2, Q_0 = 0.2$ .

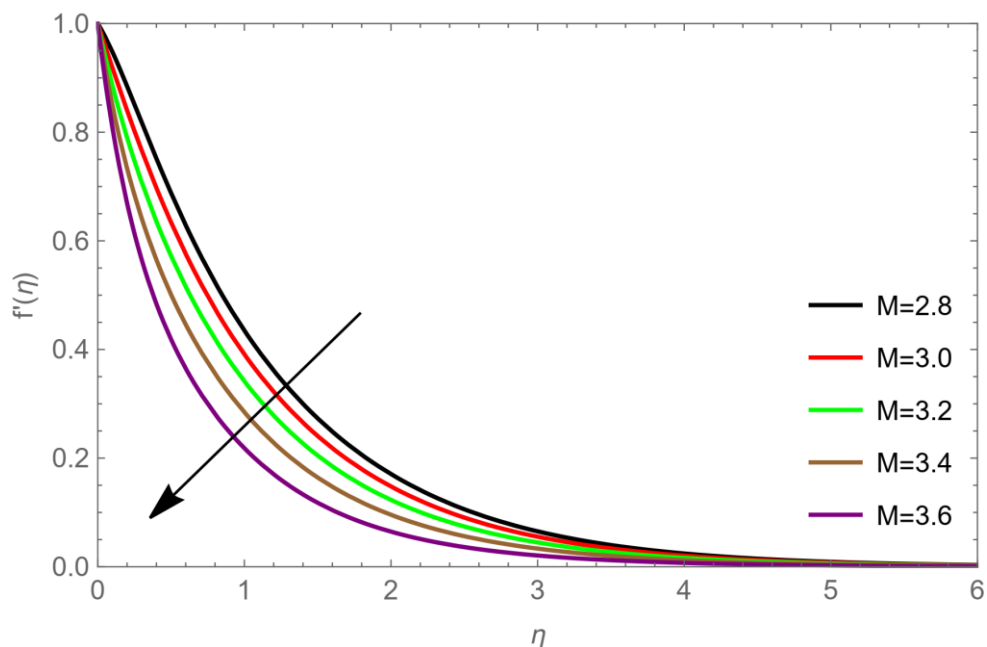


Fig. 3. Magnetic parameter ( $M$ ) effects on velocity profiles for values  $Pr = 1.0, S_c = 0.2, Nb = 0.1, Nt = 0.2, \beta = 0.2, \omega = 0.2, \lambda = 0.1, Pe = 0.3, Rd = 0.2, F_r = 0.5, L_b = 0.2, Q_0 = 0.2$ .

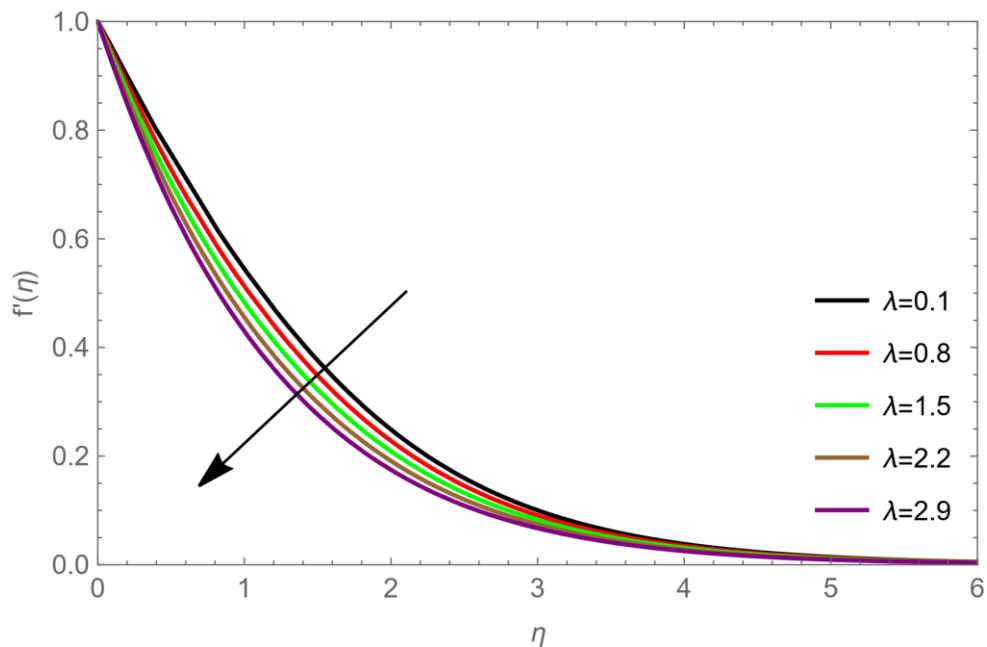


Fig. 4. Porosity parameter ( $\lambda$ ) effects on velocity profiles for values  $Pr = 1.0, S_c = 0.2, Nb = 0.1, Nt = 0.2, \beta = 0.2, \omega = 0.2, M = 0.1, Pe = 0.3, Rd = 0.2, F_r = 0.5, L_b = 0.2, Q_0 = 0.2$ .

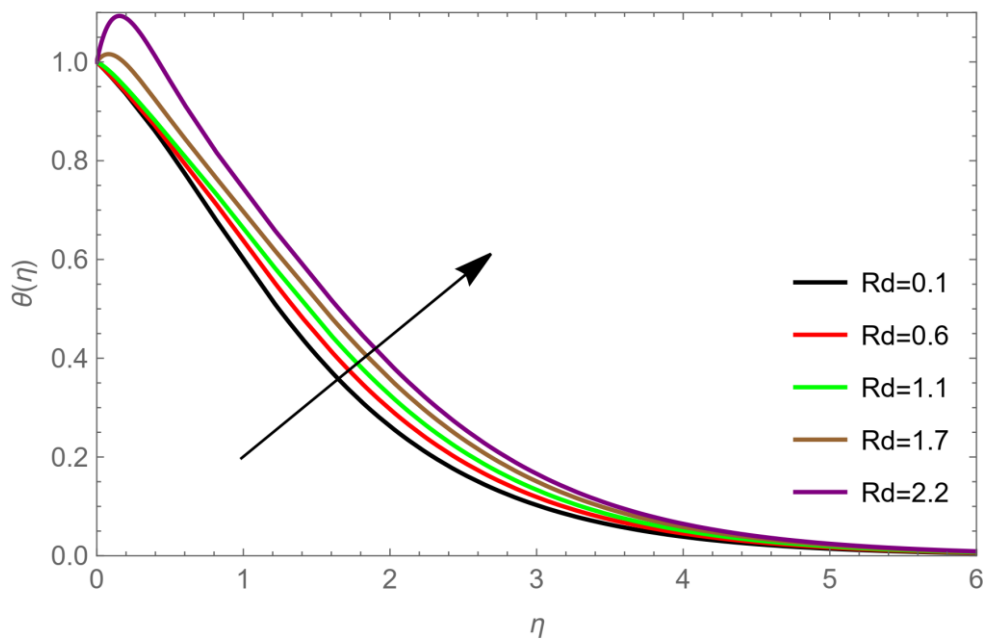


Fig. 5. Radiation parameter ( $Rd$ ) effects on temperature profiles for values  $Pr = 1.0, S_c = 0.2, Nb = 0.1, Nt = 0.2, \beta = 0.2, \omega = 0.2, M = 0.1, Pe = 0.3, \lambda = 0.1, F_r = 0.5, L_b = 0.2, Q_0 = 0.2$ .

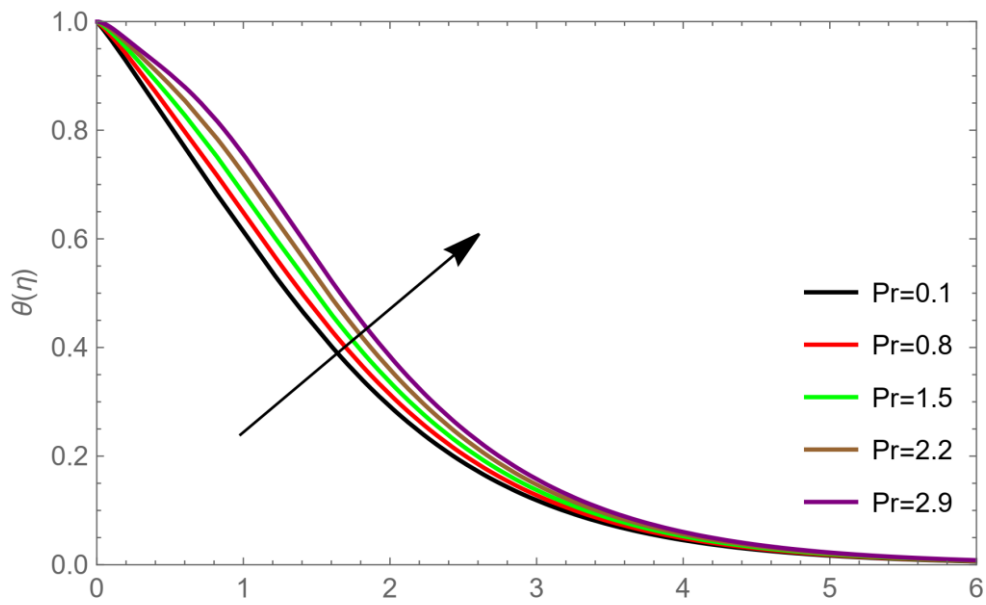


Fig. 6. Prandtl Number ( $Pr$ ) effects on temperature profiles for values  $Rd = 0.2, S_c = 0.2, Nb = 0.1, Nt = 0.2, \beta = 0.2, \omega = 0.2, M = 0.1, Pe = 0.3, \lambda = 0.1, Fr = 0.5, L_b = 0.2, Q_0 = 0.2$ .

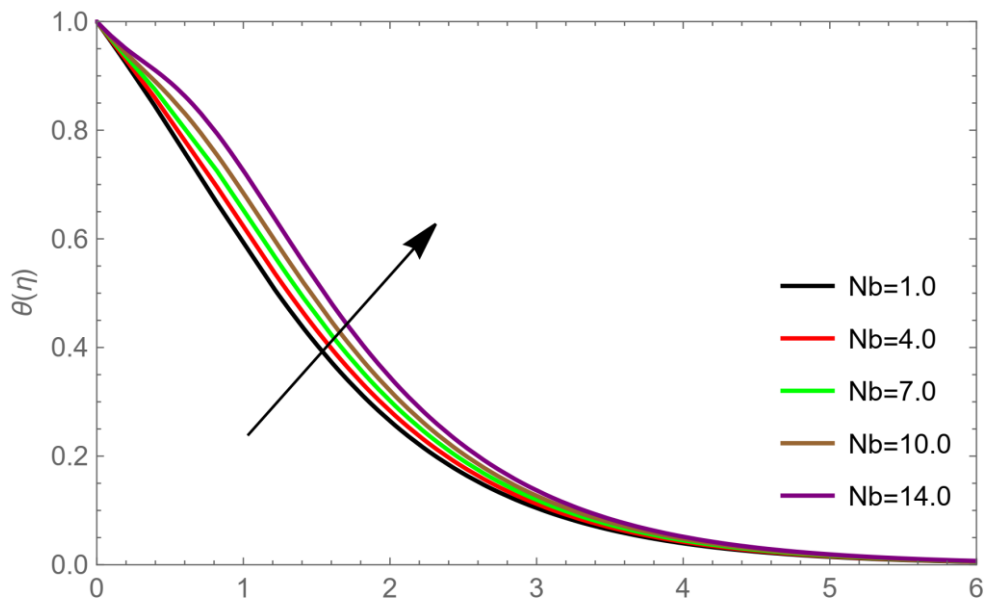


Fig. 7. Brownian motion ( $Nb$ ) effects on temperature profiles for values  $Rd = 0.2, S_c = 0.2, Pr = 1.0, Nt = 0.2, \beta = 0.2, \omega = 0.2, M = 0.1, Pe = 0.3, \lambda = 0.1, Fr = 0.5, L_b = 0.2, Q_0 = 0.2$ .



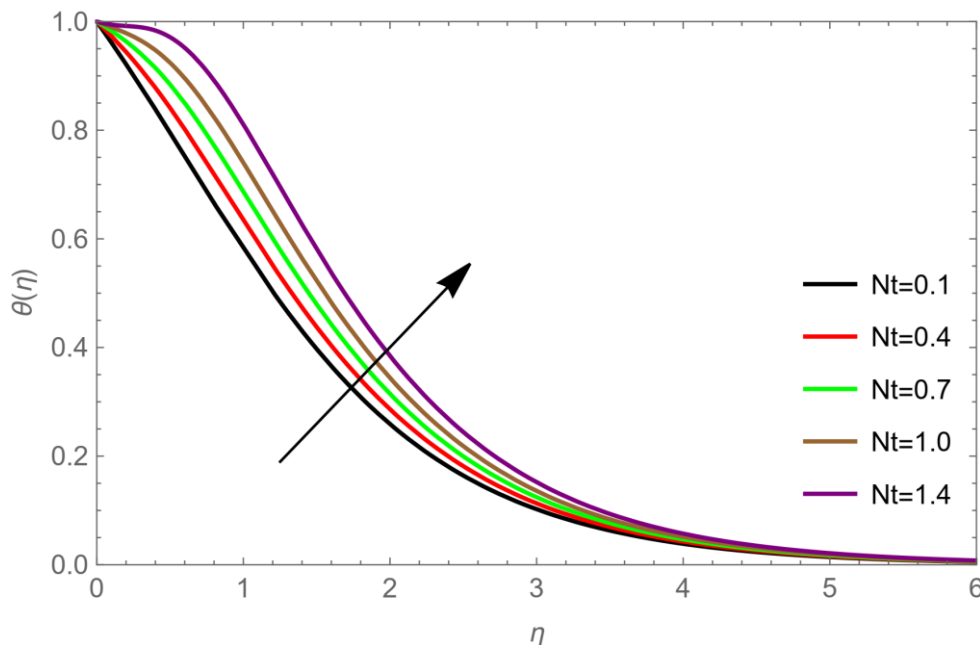


Fig. 8. Thermophoresis parameter ( $Nt$ ) effects on temperature profiles for values  $Rd = 0.2, S_c = 0.2, Pr = 1.0, Nb = 0.1, \beta = 0.2, \omega = 0.2, M = 0.1, Pe = 0.3, \lambda = 0.1, Fr = 0.5, L_b = 0.2, Q_0 = 0.2$ .

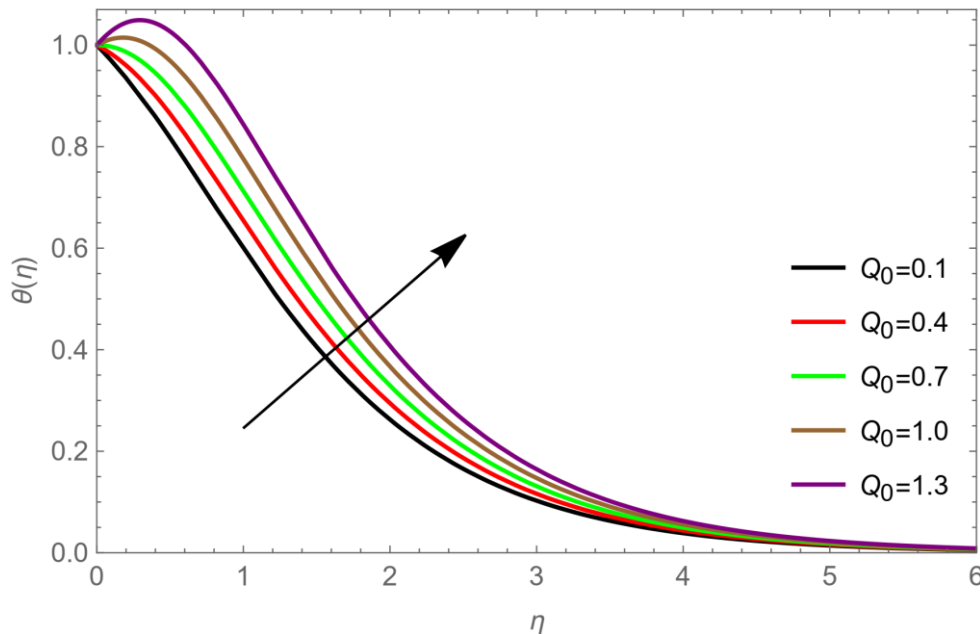


Fig. 9. Heat parameter ( $Q_0$ ) effects on temperature profiles for values  $Rd = 0.2, S_c = 0.2, Pr = 1.0, Nb = 0.1, \beta = 0.2, \omega = 0.2, M = 0.1, Pe = 0.3, \lambda = 0.1, Fr = 0.5, L_b = 0.2, Nt = 0.2$ .

The fig (5), shows temperature rises by growing radiation parameter. Effects of  $Pr$  on temperature for the chosen values is illustrated by fig (6). By increasing prandtl number the temperature profile increase. The graphs fig (7) & fig (8) demonstrate the impressions of Brownian motion  $Nb$  and thermophoresis  $Nt$ . Temperature is expected to take form like standard fluid. It is noticed by growing values of  $Nb$  &  $Nt$  have an impact on thickening the heat border layer fluid width. In fig (9), the heat parameter  $Q_0$  increase results in increase in temperature profile.

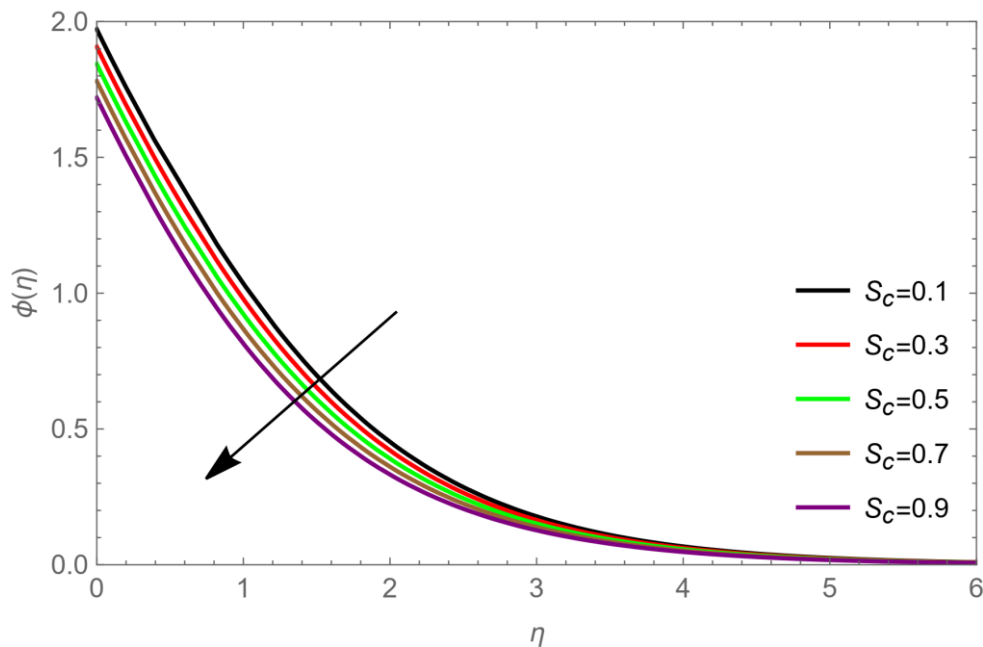


Fig. 10. Schmidt Number ( $S_c$ ) effects on concentration profile for values  $Rd = 0.2, Q_o = 0.2, Pr = 1.0, Nb = 0.1, \beta = 0.2, \omega = 0.2, M = 0.1, Pe = 0.3, \lambda = 0.1, F_r = 0.5, L_b = 0.2, Nt = 0.2$ .

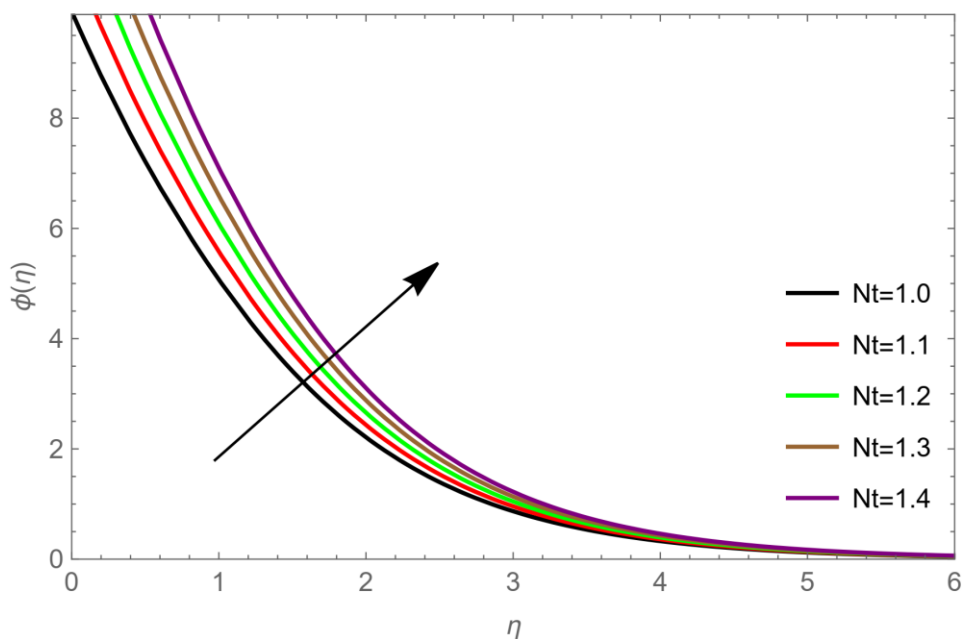


Fig.11. Thermophresis parameter ( $Nt$ ) effects on concentration profile for values  $Rd = 0.2, Q_o = 0.2, Pr = 1.0, S_c = 0.2, \beta = 0.2, \omega = 0.2, M = 0.1, Pe = 0.3, \lambda = 0.1, F_r = 0.5, L_b = 0.2, Nb = 0.1$ .

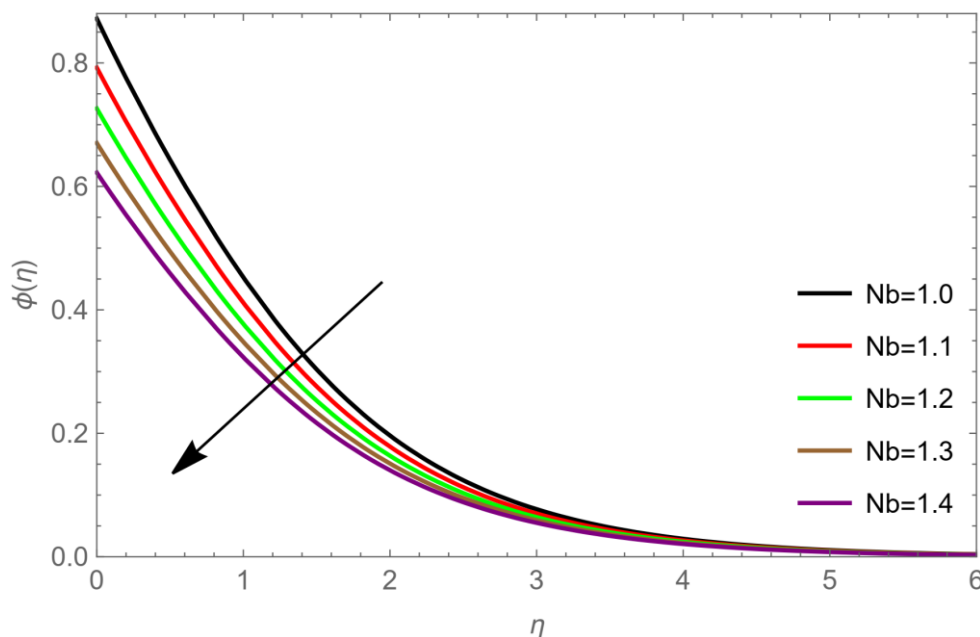


Fig. 12. Brownian motion ( $Nb$ ) effects on concentration profile for values  $Rd = 0.2, Q_o = 0.2, Pr = 1.0, S_c = 0.2, \beta = 0.2, \omega = 0.2, M = 0.1, Pe = 0.3, \lambda = 0.1, F_r = 0.5, L_b = 0.2, Nt = 0.2$ .

Impact of  $Sc$  on concentration profile is observed in fig (10). As,  $Sc$  is the relation of thermal diffusion and kinematic viscosity which results the thinning heat boundary layer of fluid wideness. So, the concentration fall by rising Schmidt number  $Sc$ . The effects of chosen values of parameter  $Nt$  &  $Nb$  observed on concentration profile in graph fig (11) and fig (12). The reverse phenomenon is shown by Brownian motion parameter on concentration of nanofluids. It is experienced that increase in nanoparticle volume portion both friction factor coefficients increase. So that's why concentration profile decrease with growth in  $Nb$  parameter values. The growth in nanofluid concentration is noted by higher values of  $Nt$  parameter.

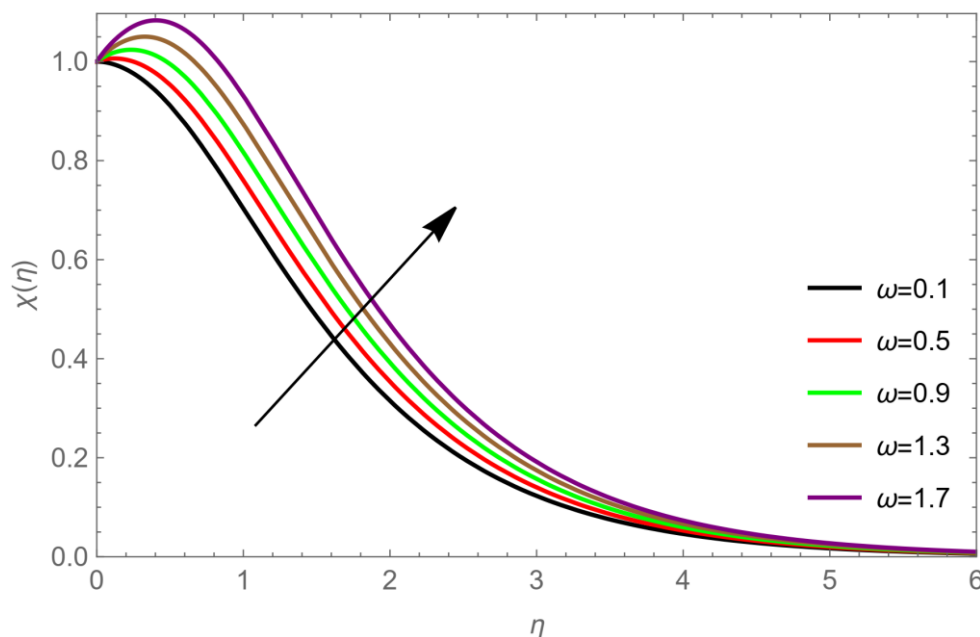


Fig. 14. Bioconvection ( $\omega$ ) effects on microorganism profile for values  $Rd = 0.2, Q_o = 0.2, Pr = 1.0, S_c = 0.2, \beta = 0.2, L_b = 0.2, M = 0.1, Pe = 0.3, \lambda = 0.1, F_r = 0.5, Nt = 0.2, Nb = 0.1$ .

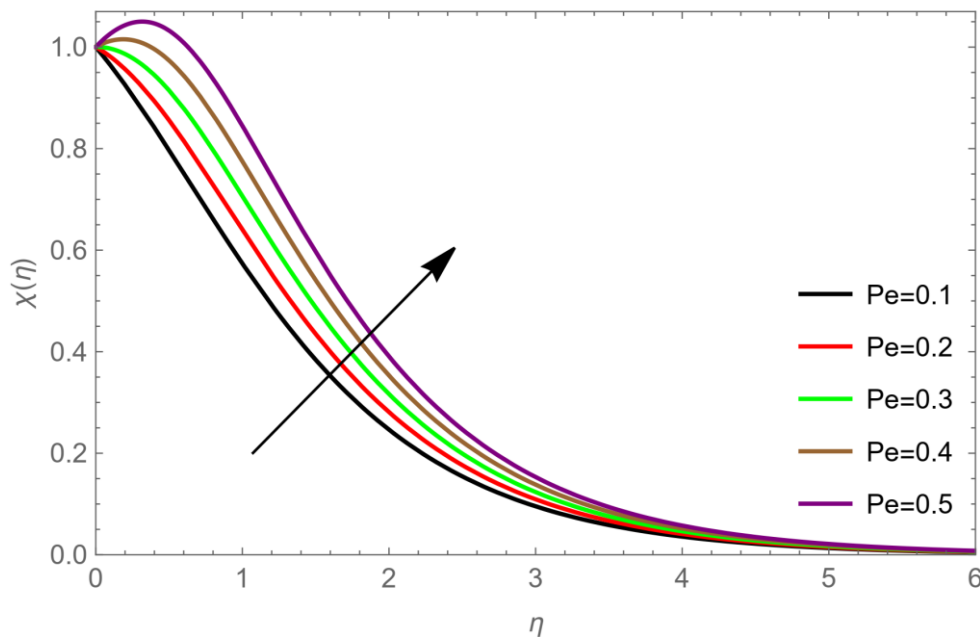


Fig. 15. Peclet number ( $Pe$ ) effects on microorganism profile for values  $Rd = 0.2, Q_o = 0.2, Pr = 1.0, S_c = 0.2, \beta = 0.2, Lb = 0.2, M = 0.1, \omega = 0.2, \lambda = 0.1, F_r = 0.5, Nt = 0.2, Nb = 0.1$ .

Fig (13) denotes the impact of  $Lb$  on microorganism profile. As  $Lb$  rise the microorganism profile decrease. The result of bioconvection and peclet number on microorganism profile is shown by fig (14) & fig (15). The microorganism profile increase with enhancing bioconvection and peclet number.

In present segment (Table 1), the impacts of  $Nt$  and  $Nb$  is noted on Nusselt number and Sherwood number. A judgment of current research values is done with previous study of (Aminreza Noghrehabad, 2012) findings.

TABLE I. ANALYSIS OF HEAT TRANSFER COEFFICIENT AND MASS TRANSFER RATE.

Nt	Nb	Aminreza Noghrehabad	Current findings	Aminreza Noghrehabad	Current findings
		$-\theta'$	$-\theta'$	$-\varphi'$	$-\varphi'$
0.1	0.1	2.1293938	2.1293889	0.9523768	0.9523645
0.2	0.1	2.2740215	2.2740115	0.6931743	0.6931236
0.3	0.1	2.5286382	2.5286234	0.5200790	0.5200237
0.4	0.1	2.7951701	2.7951598	0.4025808	0.4025648
0.5	0.1	3.0351425	3.0351543	0.3210543	0.3210413
0.1	0.2	2.3818706	2.3818678	0.5055814	0.5055345
0.1	0.3	2.4100188	2.4100023	0.2521560	0.2521467
0.1	0.4	2.3996502	2.3996419	0.1194059	0.1194013
0.1	0.5	2.3835712	2.3835587	0.0542534	0.0542534
0.2	0.3	-	2.5148519	-	0.1818823
0.3	-	-	2.6085720	-	0.1357689

In Table 2 the impacts of Casson fluid Parameter, thermophoresis ( $Nt$ ) and Brownian motion ( $Nb$ ) is observed. By growing the Brownian motion, Nusselt number decreases as well as Sherwood number declines. Also, Nusselt number decrease with the enhancement of thermophoresis parameter. The Sherwood number increase along the increment in value of  $Nt$ .

TABLE II. ANALYSIS OF DIMENSIONLESS STRESS.

Nt	$\beta=0.5, Nb=0.05$			$\beta=0.1, Nb=0.07$			$\beta=1.5, Nb=0.09$		
	$f''$	$-\theta'$	$-\varphi'$	$f''$	$-\theta'$	$-\varphi'$	$f''$	$-\theta'$	$-\varphi'$
0.03	- 0.666727675	4.444010631	2.666406379	- 0.843080242	4.423423324	1.895752853	- 0.938990309	4.412358962	1.470786321
0.05	- 0.666727675	4.246714324	4.246714324	- 0.843080242	4.226456080	3.018897200	- 0.938990309	4.215570066	2.341983370
0.07	- 0.666727675	4.060156219	5.684218707	- 0.843080242	4.040241412	4.040241412	- 0.938990309	4.029541444	3.134087790
0.09	- 0.666727675	3.883787186	6.990816934	- 0.843080242	3.864227680	4.968292732	- 0.938990309	3.853720100	3.853720100

### 5. CONCLUSION

In this research study, the impressions of thermophoresis Brownian motion and Casson fluid are analyzed and impacts of variant parameters are noted on velocity, temperature and concentration profiles. The leading equations are solved by BVP2.0 using Mathematica software. The observing results are concluded in this section by the help of numerical technique.

- Due to rise in Brownian motion, the temperature profile increase;
- There is a drop in concentration by the boost in Brownian motion but increase with thermophoresis parameter;
- The temperature improve with enhancing thermophoresis parameter’s values;
- It is conclude that Sherwood number increase with thermophoresis parameter while reverse phenomenon observed by Nb;
- The skin friction enhances with rising in Brownian motion parameter;
- By increment in thermophoresis, Brownian motion and Prandtl number, reduction in Nusselt number is observed;
- The temperature decrease with growing values of Prandtl number.

**Availability of data and material:** The data used to support this study are included in the Manuscript.

#### Nomenclature

Abbreviation	Full Name
$\beta$	Casson fluid parameter
$\alpha$	thermal diffusivity
Nb	Bronian motion parameter
Nt	thermophoresis parameter
T	fluid temperature at outer layer
$T_w$	temperature across sheet surface
$T_\infty$	temperature far away from the sheet surface
$C_w$	Concentration of nanoparticles at sheet surface
$C_\infty$	ambient nano particles concentration at boundary layer
Pr	Prandtl number
Sc	Schmidt number

$C_f$	skin friction
$Nu_x$	Nusselt number
$Sh_x$	local Sherwood number
$D_B$	Brownian diffusion
$D_T$	thermophoresis diffusion
$u_w$	velocity of stretching sheet
$k$	heat conductivity
$Re_x$	local Reynolds number
$\nu$	kinematic viscosity
$u$	x-component of velocity
$v$	y-component of velocity
$(\rho)_p$	nanoparticles heat capacity
$(\rho)_f$	fluid heat capacity
$\mu$	Dynamic viscosity of fluid
$\phi$	concentration of fluid particles
$\theta$	dimensionless temperature
$Rd$	Radiation factor
$F_r$	Local inertia
$\chi(\eta)$	Gyrotactic microorganisms
$\lambda$	Porosity factor
$\sigma$	Electric conductivity
$K_1$	Permeability
$C_b$	Inertial coefficient
$B_o$	Magnetic effect
$M$	Magnetic parameter
$W_c$	Maximum cell speed
$D_m$	Coefficient of microorganisms

$\rho$	Nanofluid density
Pe	Peclet number
$q_r$	Radiative heat flux
$\omega$	Bioconvection

### Funding

The authors present their appreciation to King Saud University for funding this research through Researchers Supporting Program number (RSPD2024R704), King Saud University, Riyadh, Saudi Arabia.

### Conflicts of interest

The paper explicitly states that there are no conflicts of interest to disclose.

### Acknowledgment

The authors present their appreciation to King Saud University for funding this research through Researchers Supporting Program number (RSPD2024R704), King Saud University, Riyadh, Saudi Arabia.

### References

- [1] N. Casson, "Flow equation for pigment-oil suspensions of the printing ink-type," *Rheology of Disperse Systems*, pp. 84-104, 1959.
- [2] J. Buongiorno, "Convective transport in nanofluids," 2006.
- [3] Z. Haddad, E. Abu-Nada, H. F. Oztop, and A. Mataoui, "Natural convection in nanofluids: Are the thermophoresis and Brownian motion effects significant in nanofluid heat transfer enhancement?" *International Journal of Thermal Sciences*, vol. 57, pp. 152-162, 2012.
- [4] M. Sheikholeslami and D. D. Ganji, "Nanofluid flow and heat transfer between parallel plates considering Brownian motion using DTM," *Computer Methods in Applied Mechanics and Engineering*, vol. 283, pp. 651-663, 2015.
- [5] T. Hayat, T. Muhammad, A. Qayyum, A. Alsaedi, and M. Mustafa, "On squeezing flow of nanofluid in the presence of magnetic field effects," *Journal of Molecular Liquids*, vol. 213, pp. 179-185, 2016.
- [6] M. J. Babu and N. Sandeep, "3D MHD slip flow of a nanofluid over a slendering stretching sheet with thermophoresis and Brownian motion effects," *Journal of Molecular Liquids*, vol. 222, pp. 1003-1009, 2016.
- [7] A. Malvandi, S. Heysiattalab, and D. D. Ganji, "Thermophoresis and Brownian motion effects on heat transfer enhancement at film boiling of nanofluids over a vertical cylinder," *Journal of Molecular Liquids*, vol. 216, pp. 503-509, 2016.
- [8] A. S. Dogonchi and D. D. Ganji, "Thermal radiation effect on the nanofluid buoyancy flow and heat transfer over a stretching sheet considering Brownian motion," *Journal of Molecular Liquids*, vol. 223, pp. 521-527, 2016.
- [9] A. Ullah, E. O. Alzahrani, Z. Shah, M. Ayaz, and S. Islam, "Nanofluids thin film flow of Reiner-Philippoff fluid over an unstable stretching surface with Brownian motion and thermophoresis effects," *Coatings*, vol. 9, no. 1, p. 21, 2018.
- [10] E. Nelson, *Dynamical Theories of Brownian Motion*, vol. 101. Princeton University Press, 2020.
- [11] M. Mustafa, T. Hayat, I. Pop, and A. Hendi, "Stagnation-point flow and heat transfer of a Casson fluid towards a stretching sheet," *Zeitschrift für Naturforschung A*, vol. 67, no. 1-2, pp. 70-76, 2012.
- [12] S. Murtaza et al., "Analysis and numerical simulation of fractal-fractional order non-linear couple stress nanofluid with cadmium telluride nanoparticles," *Journal of King Saud University-Science*, vol. 35, no. 4, p. 102618, 2023.
- [13] A. Akgül and H. Ahmad, "Reproducing kernel method for Fangzhu's oscillator for water collection from air," *Mathematical Methods in the Applied Sciences*, 2020.
- [14] H. Ahmad and T. A. Khan, "Variational iteration algorithm I with an auxiliary parameter for the solution of differential equations of motion for simple and damped mass-spring systems," *Noise & Vibration Worldwide*, vol. 51, no. 1-2, pp. 12-20, 2020.
- [15] H. Ahmad et al., "Application of novel method to withdrawal of thin film flow of a magnetohydrodynamic third grade fluid," *Ain Shams Engineering Journal*, p. 102885, 2024.

- [16] O. Ojjela, K. Ramesh, and S. K. Das, "Second law analysis of MHD squeezing flow of Casson fluid between two parallel disks," *International Journal of Chemical Reactor Engineering*, vol. 16, no. 6, 2018.
- [17] K. Rafique et al., "Energy and mass transport of Casson nanofluid flow over a slanted permeable inclined surface," *Journal of Thermal Analysis and Calorimetry*, vol. 144, pp. 2031-2042, 2021.
- [18] K. Rafique et al., "Numerical solution of Casson nanofluid flow over a non-linear inclined surface with Soret and Dufour effects by Keller-box method," *Frontiers in Physics*, vol. 7, p. 139, 2019.
- [19] M. H. Abolbashari et al., "Analytical modeling of entropy generation for Casson nanofluid flow induced by a stretching surface," *Advanced Powder Technology*, vol. 26, no. 2, pp. 542-552, 2015.
- [20] P. Sreenivasulu, T. Poornima, and N. B. Reddy, "Influence of Joule heating and non-linear radiation on MHD 3D dissipating flow of Casson nanofluid past a non-linear stretching sheet," *Nonlinear Engineering*, vol. 8, no. 1, pp. 661-672, 2019.
- [21] I. S. Oyelakin, S. Mondal, and P. Sibanda, "Nonlinear radiation in bioconvective Casson nanofluid flow," *International Journal of Applied and Computational Mathematics*, vol. 5, pp. 1-20, 2019.
- [22] S. Shaw et al., "Pulsatile Casson fluid flow through a stenosed bifurcated artery," *International Journal of Fluid Mechanics Research*, vol. 36, no. 1, 2009.
- [23] F. Shahzad et al., "Thermal analysis on Darcy-Forchheimer swirling Casson hybrid nanofluid flow inside parallel plates in parabolic trough solar collector: An application to solar aircraft," *International Journal of Energy Research*, vol. 45, no. 15, pp. 20812-20834, 2021.
- [24] R. Mehmood et al., "Non-aligned stagnation point flow of radiating Casson fluid over a stretching surface," *Alexandria Engineering Journal*, vol. 57, no. 2, pp. 939-946, 2018.
- [25] M. Tamoor et al., "Magnetohydrodynamic flow of Casson fluid over a stretching cylinder," *Results in Physics*, vol. 7, pp. 498-502, 2017.
- [26] Z. Mehmood, R. Mehmood, and Z. Iqbal, "Numerical investigation of micropolar Casson fluid over a stretching sheet with internal heating," *Communications in Theoretical Physics*, vol. 67, no. 4, pp. 443, 2017.
- [27] A. Hussain et al., "Heat transport investigation of magneto-hydrodynamics (SWCNT-MWCNT) hybrid nanofluid under the thermal radiation regime," *Case Studies in Thermal Engineering*, vol. 27, p. 101244, 2021.
- [28] B. C. Prasannakumara, "Numerical simulation of heat transport in Maxwell nanofluid flow over a stretching sheet considering magnetic dipole effect," *Partial Differential Equations in Applied Mathematics*, vol. 4, p. 100064, 2021.
- [29] N. Shukla and P. Rana, "Unsteady MHD nanofluid flow past a stretching sheet with Stefan blowing effect: HAM solution," in *AIP Conference Proceedings*, vol. 1897, no. 1, p. 020037, 2017.
- [30] M. Amjad et al., "Influence of Lorentz force and induced magnetic field effects on Casson micropolar nanofluid flow over a permeable curved stretching/shrinking surface under the stagnation region," *Surfaces and Interfaces*, vol. 21, p. 100766, 2020.
- [31] H. B. Lanjwani et al., "Stability analysis of triple solutions of Casson nanofluid past on a vertical exponentially stretching/shrinking sheet," *Advances in Mechanical Engineering*, vol. 13, no. 11, p. 16878140211059679, 2021.
- [32] B. Mahanthesh and T. V. Joseph, "Dynamics of magneto-nano third-grade fluid with Brownian motion and thermophoresis effects in the pressure type die," *Journal of Nanofluids*, vol. 8, no. 4, pp. 870-875, 2019.
- [33] F. Mabood and S. Shateyi, "Multiple slip effects on MHD unsteady flow heat and mass transfer impinging on permeable stretching sheet with radiation," *Modelling and Simulation in Engineering*, vol. 2019, 2019.
- [34] R. U. Haq et al., "Convective heat transfer and MHD effects on Casson nanofluid flow over a shrinking sheet," *Central European Journal of Physics*, vol. 12, pp. 862-871, 2014.
- [35] Z. Shah, P. Kumam, and W. Deebani, "Radiative MHD Casson nanofluid flow with activation energy and chemical reaction over past nonlinearly stretching surface through entropy generation," *Scientific Reports*, vol. 10, no. 1, p. 4402, 2020.
- [36] M. Abd El-Aziz and A. A. Afify, "MHD Casson fluid flow over a stretching sheet with entropy generation analysis and Hall influence," *Entropy*, vol. 21, no. 6, p. 592, 2019.
- [37] K. Ali et al., "Quasi-linearization analysis for entropy generation in MHD mixed-convection flow of Casson nanofluid over nonlinear stretching sheet with Arrhenius activation energy," *Symmetry*, vol. 14, no. 9, p. 1940, 2022.
- [38] P. G. Metri, M. S. Abel, and D. S. Sharanappa, "Magnetohydrodynamic Casson nanofluid flow over a nonlinear stretching sheet with velocity slip and convective boundary conditions," in *Stochastic Processes, Statistical Methods, and Engineering Mathematics: SPAS 2019*, Västerås, Sweden, September 30–October 2, Cham: Springer International Publishing, pp. 773-789, 2023.



- [39] B. Souayah et al., "Comparative analysis on non-linear radiative heat transfer on MHD Casson nanofluid past a thin needle," *Journal of Molecular Liquids*, vol. 284, pp. 163-174, 2019.
- [40] S. Nadeem et al., "MHD three-dimensional Casson fluid flow past a porous linearly stretching sheet," *Alexandria Engineering Journal*, vol. 52, no. 4, pp. 577-582, 2013.
- [41] F. Wang et al., "Activation energy on three-dimensional Casson nanofluid motion via stretching sheet: Implementation of Buongiorno's model," *Journal of the Indian Chemical Society*, p. 100886, 2023.
- [42] S. Nadeem, R. U. Haq, and N. S. Akbar, "MHD three-dimensional boundary layer flow of Casson nanofluid past a linearly stretching sheet with convective boundary condition," *IEEE Transactions on Nanotechnology*, vol. 13, no. 1, pp. 109-115, 2013.
- [43] G. Mahanta and S. Shaw, "3D Casson fluid flow past a porous linearly stretching sheet with convective boundary condition," *Alexandria Engineering Journal*, vol. 54, no. 3, pp. 653-659, 2015.
- [44] C. Sulochana, G. P. Ashwinkumar, and N. Sandeep, "Similarity solution of 3D Casson nanofluid flow over a stretching sheet with convective boundary conditions," *Journal of the Nigerian Mathematical Society*, vol. 35, no. 1, pp. 128-141, 2016.
- [45] W. Ibrahim and O. D. Makinde, "Magnetohydrodynamic stagnation point flow and heat transfer of Casson nanofluid past a stretching sheet with slip and convective boundary condition," *Journal of Aerospace Engineering*, vol. 29, no. 2, p. 04015037, 2016.
- [46] V. Makkar, V. Poply, and N. Sharma, "Three dimensional modelling of magnetohydrodynamic bio-convective Casson nanofluid flow with buoyancy effects over exponential stretching sheet along with heat source and gyrotactic micro-organisms," *Journal of Nanofluids*, vol. 12, no. 2, pp. 535-547, 2023.
- [47] M. Sohail et al., "Utilization of updated version of heat flux model for the radiative flow of a non-Newtonian material under Joule heating: OHAM application," *Open Physics*, vol. 19, no. 1, pp. 100-110, 2021.
- [48] T. Naseem et al., "Numerical exploration of thermal transport in water-based nanoparticles: A computational strategy," *Case Studies in Thermal Engineering*, vol. 27, p. 101334, 2021.
- [49] U. Nazir et al., "Effective role of mineral oil and biological nanomaterial on thermal energy influenced by magnetic dipole and nanoparticle shape," *Frontiers in Materials*, vol. 10, p. 1107661, 2023.
- [50] R. Naz, M. Sohail, and T. Hayat, "Numerical exploration of heat and mass transport for the flow of nanofluid subject to Hall and ion slip effects," *Multidiscipline Modeling in Materials and Structures*, vol. 16, no. 5, pp. 951-965, 2020.